Vegetation, sea-level and climate changes during the Messinian salinity crisis

Gonzalo Jiménez-Moreno[a, *], **José Noel Pérez-Asensio**[a], **Juan Cruz Larrasoaña**[b], **Julio Aguirre**[a], **Jorge Civis**[c], **María Rosario Rivas-Carballo**[c], **María F. Valle-Hernández**[c], **José Angel González-Delgado**[c]

[a]Departamento de Estratigrafía y Paleontología, Universidad de Granada, Fuente Nueva s/n, 18002, Granada, Spain.

[b] Instituto Geológico y Minero de España, Unidad de Zaragoza, C/ Manuel Lasala 44, 9B, 50006, Zaragoza, Spain

[c] Departamento de Geología, Universidad de Salamanca, Plaza de la Merced S/N, 37008, Salamanca, Spain

* Corresponding author: Tel.: +34-958248727;
Fax: +34-958-248528
E-mail address: gonzaloj@ugr.es

ABSTRACT

The Messinian salinity crisis (MSC; Late Miocene) is one of the most fascinating paleoceanographic events in the recent geological history of the Mediterranean Sea - it went through partly or nearly complete desiccation. However, the relative role that tectonic processes and sea level changes had, as triggers for restriction and isolation of the Mediterranean Sea from the open ocean, is still under debate. In this study we present a detailed pollen, dinoflagellate cyst (dinocyst) and magnetic susceptibility analysis of a sequence of late Neogene (between ca. 7.3 to 4.1 Ma) marine sediments from the Montemayor-1 core (lower Guadalquivir Basin, southwestern Spain), which provides a continuous record of paleoenvironmental variations in the Atlantic side of the Betic corridors during the Late Miocene. Our results show that significant paired vegetation and sea level changes occurred during the Messinian likely triggered by orbital-scale climate change. Important cooling events and corresponding glacio-eustatic sea-level drops are observed in this study at ca. 5.95 and 5.80 Ma coinciding with the timing and duration of oxygen isotopic events TG32 and TG22-20 recorded in marine sediments worldwide. It is generally accepted that the onset of the MSC begun at ca. 5.96 ± 0.02 Ma. Therefore, this study suggests that the restriction of the Mediterranean could have been triggered, at least in part, by a strong glacio-eustatic sea level drop linked to a climate cooling occurring at the time of the MSC initiation.

INTRODUCTION

In the last decades a great effort has been made to understand the role of tectonic and climatic processes as drivers of the Messinian Salinity Crisis (MSC). First, glacio-eustatic changes were assumed as a trigger for the restriction of the Mediterranean (Kastens, 1992; Hodell et al., 1994; Clauzon et al., 1996; Zhang and Scott, 1996; Rouchy and Caruso, 2006). Glacial oxygen isotopic stages TG22-20, observed in many marine records (Hodell et al., 1994; Shackleton et al., 1995), were often suggested to have produced a significant (ca. 50 m) glacio-eustatic drop restricting the Mediterranean from the Atlantic Ocean.

However, other studies have pointed to tectonics as the main cause that triggered the restriction of the Mediterranean (Weijermars, 1988; Braga and Martín, 1992; Martín and Braga, 1994, 1996; Krijgsman et al., 1999a; Hodell et al., 2001; Vidal et al., 2002; Hilgen et al., 2007; Govers, 2009). This interpretation stems from the observation that the beginning of the MSC at 5.96 ± 0.02 Ma (Krijgsman et al., 1999a), dated by precessional cycle counting, preceded the above mentioned glacio-eustatic sea-level drop (sequence boundary Me-2; Hardenbol et al, 1998) that occurred at ca. 5.75 Ma during isotope stages TG22-20. As other significant cold isotopic events are recorded previous to 5.75 Ma (i.e., ca. 5.95 and 6.25 Ma; Shackleton and Hall, 1997; Shackleton et al., 1999; Vidal et al., 2002), the question of whether their associated glacio-eustatic sea-level drops might have triggered restriction of the Mediterranean remains open.

Previous pollen studies in Messinian marine sediments from the Mediterranean area (see synthesis in Fauquette et al., 2006) show changes mostly characterized by variations in *Pinus* content. These changes were interpreted as being controlled by eustatic fluctuations, not pointing to climate, as *Pinus* concentration usually increases with the distance to coast (Fauquette et al., 2006). Climate estimates derived from these pollen data do not show any obvious climatic changes during or after the restriction of the Mediterranean Sea, thereby suggesting that climate was not the direct cause of the MSC (Fauquette et al., 2006). However, reports of a major cooling episode and increase in global ice volume in the late Miocene are widespread, marked with numerous glacial-to-interglacial oscillations (see Hodell et al., 2001; Vidal et al., 2002).

In this study we present new pollen, dinocyst and magnetic susceptibility data from the Montemayor-1 borehole, which provides a continuous record of paleoenvironmental variations in the Atlantic side of the Gibraltar Arch during the Late Miocene. These data demonstrate cyclic and paired changes in vegetation and sea level that appear to be linked to climate (i.e., “glacial-interglacial”) variability. They therefore enable reassessment of the role of sea-level variations as triggers for the restriction and isolation of the Mediterranean-Atlantic connection.

STUDY AREA

The Guadalquivir Basin in southern Spain is an ENE-WSW elongated foreland basin that developed during the Neogene between the external units of the Betic Cordillera to the south and the Sierra Morena (Iberian Massif) to the north (Sanz de Galdeano and Vera, 1992; Braga et al., 2002) (Fig. 1). The Guadalquivir Basin started to develop during the Middle Miocene in response to flexural subsidence of the Iberian Massif, which was in turn caused mainly by the Early-Middle Miocene stacking of allocthonous units of the external Betics during the NW-directed convergence between the Eurasian and African plates (Sierro et al., 1996; Fernández et al., 1998; González-Delgado et al., 2004; Aguirre et al., 2007; Martín et al., 2009; Braga et al., 2010). Such stacking of allochthonous units led to closure of the so-called North Betic Strait during the lowermost Early Tortonian (Aguirre et al., 2007; Martín et al., 2009; Braga et al., 2010), after which the basin developed as a marine embayment opened to the Atlantic Ocean (Martín et al., 2009). The marine sedimentary infilling of the Guadalquivir Basin consists of early Tortonian-late Pliocene deposits (Aguirre, 1992, 1995; Aguirre et al., 1995; Sierro et al., 1996; Riaza and Martínez del Olmo, 1996). The progressive infilling produced a WSW-directed migration of the depocenter, approximately along its longitudinal axis. The early Tortonian to early Pliocene marine sedimentary sequence in the western part of the basin (so-called lower Guadalquivir Basin) consists of four lithostratigraphic units formally described as formations (Civis et al., 1987; Sierro et al., 1996; González-Delgado et al., 2004). The lowermost unit is the Niebla Formation (Civis et al., 1987; Baceta and Pendón, 1999), which is made up by about 30 m of late Tortonian (Civis et al., 1987) carbonate-siliciclastic mixed coastal deposits that unconformably onlap the Paleozoic-Mesozoic basement of the Iberian Massif (Baceta and Pendón, 1999). The second unit, latest Tortonian-Messinian according to planktonic foraminifera and calcareous nannoplankton (Sierro, 1985, 1987; Flores, 1987; Sierro et al., 1993), is the Arcillas de Gibraleón Formation (Civis et al., 1987), which begins with 2-4 m of glauconitic silts (Baceta and Pendón, 1999) and consists mostly of greenish-bluish clays accumulated in a deep marine through formed at the foothill of the Betic Cordillera. The third unit is the Arenas de Huelva Formation, which begins with a 3 m-thick glauconite-rich layer and includes early Pliocene silts and highly fossiliferous sands accumulated in a shallow marine environment (Civis et al., 1987). This formation is unconformably overlain by sands of the Arenas de Bonares Formation (Mayoral and Pendón, 1987), which has an early Pliocene age (Salvany et al., 2011). This marine sedimentary succession, which is overlain by a late Pliocene to Holocene sequence of mainly continental deposits (Salvany et al., 2011), has been divided into five depositional sequences (A-E) that have been correlated with third-order cycles of the Haq et al. (1987) global sea-level curve (Sierro et al., 1996).

MATERIALS AND METHODS

The 260-m-long Montemayor-1 (MTMY-1) core was drilled in the vicinity of Moguer in the northwestern margin of the lower Guadalquivir Basin (37º 16’ N 6º 49’ W; 52 m elevation; Fig. 1). Larrasoaña et al. (2008) described the core, currently curated at the Universidad de Salamanca (Spain).

The MTMY-1 core chronology was developed from a combination of biostratigraphic data coming from planktonic foraminiferal events and magnetostratigraphy (Table 1; Fig. 2; see Larrasoaña et al., 2008 for a detailed explanation). Our chronology for most of the core consists of linear interpolation between adjacent ages, using the astronomically tuned Neogene time scale (ATNTS2004) of Lourens et al. (2004).

Samples (2 cm^3) for pollen and dinoflagellate cyst (dinocyst) analyses were taken every 2.5 m throughout the core (Fig. 3), with a total of 88 samples analyzed. The palynomorph extraction method followed a modified Fægri and Iversen (1989) methodology. Counting was performed at 400 and 1000x magnifications to a minimum pollen sum of 300 terrestrial pollen grains. Fossil pollen was compared with their present-day relatives using published keys. The raw counts were transformed to pollen percentages based on the terrestrial sum, not including *Pinus*, as it is usually overrepresented in marine environments. This is because of the advantage of bisaccate pollen for long-distance transport (Heusser, 1988; Jiménez-Moreno et al., 2005). The pollen zonation was accomplished using CONISS (Grimm, 1987). Dinocycts co-occur with the pollen in the studied slides. They were counted and classified and their percentage was calculated with respect to the total terrestrial pollen sum. The dinocyst/pollen ratio [d/p ratio = (d-p)/(d+p)] was also calculated (Fig. 4).

A cyclostratigraphic analysis was performed on the 5-6.5 Ma interval of the MTMY-1 percentage of *Quercus* pollen. We used the program REDFIT (Schulz and Mudelsee, 2002) with the objective of characterizing the different periodicities present in the unevenly spaced time series and estimating their red-noise spectra. The spectral analysis assisted in identifying recurrent features or periodicities through spectral peaks registered at differing frequencies throughout the studied core. A sinusoidal curve fitting, using PAST (Hammer et al., 2001) was also run on the *Quercus* percentages.

Low-field magnetic susceptibility was measured on 120 standard paleomagnetic specimens using an AGICO KLY-2 susceptibility meter at the Paleomagnetic Laboratory of the IES "Jaume Almera" (CSIC-UB) in Barcelona (Spain) (Fig. 2). Paleomagnetic sampling at a mean resolution of 2 meters was done perpendicular to the core sections using a standard petrol-powered drill machine. The low field magnetic susceptibility is given normalized by the volume of the specimens (κ) (no significant change is observed by normalizing by mass), and is taken as a first order proxy for the concentration of magnetic minerals (i.e., Evans and Heller, 2003). κ is referred hereafter as MS. The intensity of the Natural Remanent Magnetization (NRM), measured using a 2G cryogenic magnetometer at the IES "Jaume Almera" (CSIC-UB), has also been used as an additional first order indicator for the concentration of magnetic minerals. A correlation analysis has been run between the MS and the d/p ratio in order to evaluate the relationship between both proxies (Fig. 5).

RESULTS

Lithology and chronology

The four marine sedimentary formations described in the study area (see section 2) have been identified in the MTMY-1 core above 1.5 m of reddish clays belonging to the Paleozoic-Mesozoic bedrock (Fig. 2). The Niebla Formation is represented by a well cemented, 0.5 m-thick sandy calcarenite layer that unconformably overlies the basement. The sequence continues with 198 m of silts and clays that belong to the Arcillas de Gibraleón Formation. The lowermost 3 m of this formation are very rich in glauconite, and can be correlated with the unconformity identified between the Niebla and Gibraleón formations in outcrop (Baceta and Pendón, 1999). The Gibraleón Formation is overlain by 42 m of sands and silts from the Arenas de Huelva Formation, whose lowermost 3 m constitute a distinctive, glauconite-rich interval. The MTMY-1 core tops with the Arenas de Bonares Formation, 14.5 m of brownish sands containing marine fossils, and 3.5 m of recent soil (Fig. 2).

Planktonic foraminiferal events 3, 4 and 6 of Sierro et al. (1993) and 11 polarity intervals (labelled N1 to N5 and R1 to R6 for normal and reversed intervals from bottom to top, respectively) have been identified in the MTMY-1 core (Fig. 2; Table 1; Larrasoaña et al., 2008). The pattern of magnetic reversals and the position of the planktonic foraminiferal events enable a fairly good correlation to the ATNTS, which provides robust age estimates for the late Miocene part of the core (Fig. 2). Thus, our correlation suggests a latest Tortonian age (C3Br.2r, ca. 7.4-7.3 Ma) for the Niebla Formation and a latest Tortonian to latest Messinian age (topmost of C3Br.2r to C3r/C3n boundary; ca. 7.3 to 5.25 Ma) for the Gibraleón Formation. A less clear correlation is obtained for the uppermost part of the core (Pérez-Asensio et al., 2012). The appearance of *G. puncticulata* is found near the N5/R6 boundary in the MTMY-1 core. In view of the straightforward correlation of R5 with chron C3r, and keeping in mind the age of the appearance of *G. puncticulata* (4.52 Ma near the top of C3n.2n

(Lourens et al., 2004), the most conservative interpretation is to infer a discontinuity spanning most of the lower part of chron C3n (subchrons 2n to 4n) and probably also the topmost part of chron C3r (Pérez-Asensio et al., 2012). In view of the occurrence of the glauconite-rich interval at the base of the Huelva Fm, the most likely interpretation is that the discontinuity involves very low accumulation rates in the lowermost part of the Pliocene (Larrasoaña et al., 2008). Therefore, according to these authors, it is reasonable to assume that the Messinian record is almost complete. Age estimates for all the studied samples from the MTMY-1 core were assigned by assuming linear accumulation rates between the age tie-points represented by the (sub)chron boundaries.

Pollen and dinocysts

Ninety different pollen species have been identified in the MTMY-1 core. The record shows a very rich and diverse flora, although most of the identified taxa occur in percentages lower than 1% (not plotted in Figure 3). These rare species include thermophilous plants such as *Avicennia* (only two occurrences at ca. 6.4 and 5.5 Ma), Taxodiaceae, *Engelhardia*, *Platycarya*, *Myrica*, Rutaceae, Chloranthaceae, *Acacia*, Sapotaceae or Celastraceae. Temperate tree species are also diversified but most of them occur in very low percentages (i.e., *Fagus*, *Carya*, *Juglans*, *Liquidambar* and *Alnus*), except for *Quercus* (see below).

The pollen record from the MTMY-1 core shows high percentages of *Pinus* varying around 50%, and is characterized by high-percentages of herbs (mostly Lactucaceae, Asteraceae, Amaranthaceae) and grasses (Poaceae). Non-coniferous trees are less abundant and are mostly dominated by evergreen and deciduous *Quercus*.

We used variations in pollen species (excluding *Pinus*, see reasons above) to objectively zone the pollen data using the program CONISS (Grimm, 1987), producing eight pollen zones for the MTMY-1 record (Fig. 3). These data provide a general framework for discussion of vegetation change during the late Miocene around the SW Guadalquivir Basin.

Pollen zones 2, 4 and 6 are characterized by relatively high percentages in *Quercus* and dinocysts. On the other hand, during the deposition of zones 1, 3, 5 and 7, herbs and grasses dominate the pollen assemblages and relatively lower percentages in *Quercus* and dinocysts are recorded. Pollen zone 7 is mostly depicted by high percentages in Lactucaceae, Poaceae and Cupressaceae, relatively low percentages in *Quercus* and the low percentages of dinocysts. A significant decrease in *Pinus* and dinocysts is observed during pollen zone 8.

The d/p ratios generally covary with pollen changes, pollen zones 2, 4 and 6 being characterized by relatively high values. There is a significant decrease in the d/p ratios during pollen zones 7 and 8.

Periodicity of pollen changes

The MTMY-1 pollen record shows well-defined cycles superimposed on long-term late Miocene and Pliocene regional trends. The cyclostratigraphic analysis on the raw pollen data (*Quercus* total) documents statistically significant (above the 80 and 90% confidence level) periodicities between 400-200, 105, 74 and 43 ka (Fig. 6). The sinusoidal curve fitting on the *Quercus* pollen data shows that a 400 ka sinusoid optimally fits the data (Fig. 6).

Magnetic susceptibility

Magnetic susceptibility (MS) values show important variations throughout the core (Fig. 2). In the lowermost 50 m of the record (ca. 7.35 – 5.95 Ma), MS oscillates between 1000 and 2000 x 10^{-6} SI but in some samples clustering at around 235 and 255 m, where values of around 600 x 10^{-6} SI are found. This interval is characterized by highest NRM intensities. The rapid drop (down to 600-800 x 10^{-6} SI) of MS observed at around 207 m (ca. 5.95 Ma) is mirrored by a sharp decrease in the NRM intensity. The rest of the Gibraleón Formation (5.95 – 5.23 Ma) is characterized by rather constant MS values of around 750 x 10^{-6} SI and by a recovery of NRM intensities. Sediments from the Huelva Formation are characterized by lowest NRM intensities and by much lower MS values that progressively decrease from around 400 to 100 x 10^{-6} SI. It is worth noticing that there is a good correlation between the d/p ratios and MS (Fig. 5).

DISCUSSION

Pollen analysis in marine sediments is a good proxy for vegetation change inland and, thus, climate change (Heusser, 1983, 1988; Zheng et al., 2007). Thus detailed palynological studies on continuous marine sequences have shown the highly sensitive response of pollen records, tracking changes on the vegetation related to rapid millennial-scale climate variability (Fletcher et al., 2007; 2010; Fletcher and Sánchez Goñi, 2008; Sánchez Goñi et al., 2008). The pollen analysis from the MTMY-1 core agrees with previous Messinian pollen records from southern Spain and northern Morocco (Suc and Bessais, 1990; Suc et al., 1995; Fauquette et al., 2006; Jiménez-Moreno et al., 2010). Besides the overrepresentation of *Pinus*, herbs (including rare subdesertic species such as *Lygeum*, *Neurada* and *Nitraria*) dominated the vegetation during the Messinian in this area (Fig. 3). Trees were less abundant and were mostly represented by *Quercus* species. These pollen data indicate overall arid climate and open vegetation environments. Occurrences of thermophilous species such as *Avicennia*, *Engelhardia* or *Taxodiaceae*, also point to a subtropical climate. Fauquette et al. (2006)

estimated mean annual temperatures around 20-22ºC and mean annual precipitations between 450-500 mm for the Messinian in this area.

Increases and decreases in tree species (i.e., *Quercus*) during the Messinian have been interpreted as indicating forest development during relatively humid periods and contractions during more arid periods, respectively (Jiménez-Moreno et al., 2010). Similar responses of the vegetation, with *Quercus* peaking during warm-humid events (i.e., interglacials or interstadials) are observed in late Pleistocene and Holocene sediments from this area (Fletcher et al., 2007; 2010; Fletcher and Sánchez Goñi, 2008; Sánchez Goñi et al., 2008). Also, thermophilous (subtropical) species are very sensitive to temperature change and have been used in many studies for Miocene climate reconstructions (i.e., Jiménez-Moreno et al., 2005; 2008). Therefore, in this study we use *Quercus* and thermophilous taxa abundances as proxies for temperature and precipitation (Fig. 4).

The dinocyst/pollen ratio (d/p ratio) has been proved to be a good proxy for eustatic oscillations (Warny et al., 2003; Jiménez-Moreno et al., 2006; Iaccarino et al., 2008). This is because pollen, coming from the continent, decreases with the distance to shore. In the case of the MTMY-1 core, the reliability of the d/p ratio as a proxy for sea-level changes is supported by the striking similarity observed between this ratio and sea-level estimates based on benthic foraminiferal assemblages (Pérez-Asensio et al., 2012).

It is typically considered that variations in the MS of sediments and rocks with MS values larger than 500 x 10^{-6} SI and lower than 300 x 10^{-6} SI are modulated by the concentration of ferromagnetic and paramagnetic minerals, respectively (Rochette, 1987), with intermediate values indicating a mixture of ferromagnetic and paramagnetic minerals. The MS of clayey sediments from the Gibraleón Formation ranges between 1000-2000 x 10^{-6} SI and 600-800 x 10^{-6} SI below and above metre 208, respectively, whereas that of fossil-rich clayey sands from the Huelva Formation ranges between 150-400 x 10^{-6} SI. These values therefore point to a progressive decrease in the concentration of magnetite, which is the main magnetic carrier in the studied sedimentary sequence (Larrasoaña et al., 2008). This is further supported by the overall covariance observed between MS and the NRM intensity (Fig. 2).

The good linear correlation (R^2 = 0.795) between MS and the d/p ratio (Fig. 5) indicates that higher and lower concentrations of magnetite are linked to higher and lower sea levels, respectively. The most likely explanation for this circumstance is that detrital magnetite is diluted by quartz- and clay-rich terrigenous material, whose impact at the studied site increases with lower sea-level and, hence, a closer proximity to the continent. Southwest progradation of terrigenous systems along the axial part of the Guadalquivir Basin, filling up the basin (Sierro et al., 1996), would account for the important increase in the sedimentation rate in a context of sea level lowering along the MTMY-1 core (Pérez-Asensio et al., 2012). An alternative explanation could be that increased sedimentation rates and the concomitant increase in terrigenous supply, which prevents downwards migration of oxygen from the sediment-water interface (e.g. Roberts and Turner, 1993), might have driven enhanced reductive dissolution of magnetite. Nonetheless, benthic foraminiferal assemblages suggest moderate- to well-oxygenated bottom and interstitial waters (Pérez-Asensio et al., 2012). Therefore this hypothesis is less likely to produce the above-mentioned variations.

Latest Tortonian-earliest Messinian (ca. 7.3 – 7.0 Ma)

The MTMY-1 record begins with cold and arid climate conditions (pollen zone 1), deduced by very low percentages of *Quercus* and thermophilous taxa and the abundance of herbs (Figs. 3 and 4). This also corresponds in this record with a relatively low sea level, depicted by the d/p ratio, and low MS at ca. 7.3 Ma. A cold period agrees with eccentricity minima recorded at that time (Laskar et al., 2004; Fig. 4). Furthermore, the sediments recorded in the MTMY-1 core contain 44% of sand and inner-middle shelf benthic foraminifera indicating a shallow-water environment (Pérez-Asensio et al., 2012).

The isotopic record from the Salé Briqueterie Site (NW Morocco) also shows cooling at the Tortonian-Messinian boundary, with increases in $\delta^{18}O$ of benthic foraminifera related to increase in global ice volume (Hodell et al., 1994). Following these authors, the associated sea-level drop produced the restriction of the Rifian Corridor, lead to water circulation changes, and contributed to the establishment of a negative water budget in the Mediterranean. The same trend has been observed in the $\delta^{18}O$ isotopic record of the Sorbas Basin, a marginal basin in the western Mediterranean (Sánchez-Almazo et al., 2001; Martín et al., 2010). A sea-level drop at that time agrees with Agustí et al. (2006), who observed a significant turnover in murid rodents in southern Spain, probably due to this climate change.

D/p ratios and MS values mark a transgressive-regressive cycle between 7.3 – 7.0 Ma that culminates in a sea-level drop, at ca. 7.0 Ma. The transgression around the Tortonian-Messinian boundary is also recorded by a sharp decrease in the sand content, and changes in the benthic foraminiferal assemblages in the MTMY-1 core (Pérez-Asensio et al., 2012). This is most likely related to a global glacio-eustatic sea-level drop at ca. 7 Ma (Tor3/Me1 sequence boundary; Handerbol et al., 1998; Fig. 4). Pollen does not show this climatic oscillation and cold and arid climate conditions seem to persist during the above-mentioned period. Multiple evidences indicate cold (i.e., glacial) conditions at about 7 Ma in the northern and southern hemisphere (Larsen et al., 1994; Shackleton and Hall, 1997; Zachos et al., 2001; Lear et al., 2003).

Early Messinian (ca. 7.0 – 5.95 Ma)

A relatively rapid warming and a concomitant transgression are evidenced between 7.0 – 6.8 Ma in the pollen data, d/p ratios and MS values from MTMY-1 core. This coincides with a global sea-level rise (Handerbol et al., 1998; Fig. 4) and relatively low global ice volume (Shackleton and Hall, 1997; Vidal et al., 2001).

Relatively warm and humid conditions and high sea level are recorded between ca. 6.8 – 6.5 Ma (Fig. 4). This agrees with a maximum flooding surface that is observed in the carbonate platforms from the western and Central Mediterranean at ca. 6.7 Ma (Martín and Braga, 1994, 1996; Sánchez-Almazo et al., 2001, 2007; Martín et al., 2010; Cornée et al., 2004). A sea-level drop is then observed, starting at ca. 6.6 Ma in both d/p ratios and MS values, so that minimum values are recorded between ca. 6.4 – 6.3 Ma. Temperatures also decreased, reaching a minimum at ca. 6.3 Ma (Fig. 4). This agrees with regional eustatic data from Sierro et al. (1996) for the Guadalquivir Basin, and is consistent with the 4th order sea level drop identified at that time by Esteban et al. (1996) in the western Mediterranean (Fig. 4). Isotopic records also indicate an increase in global ice volume and a sea level drop at that time, which could have caused restriction and maybe even the closure of the Rifian Corridors (Hodell et al., 2001; Vidal et al., 2002), and thus the intensification of micromammal terrestrial exchanges between Africa and Iberia (Agustí et al., 2006). Contemporaneous restriction is also observed in sedimentary sequences from Sicily, the Apennines and Gavdos Basin (Caruso, 1999; Bellanca et al., 2001; Blanc-Valleron et al., 2002).

A climate-warming and more humid trend is then observed starting at ca. 6.3 Ma and reaching a maximum at ca. 6 Ma, as shown by the increase in thermophilous taxa and highest percentage of *Quercus* in the MTMY-1 core. This warming is accompanied by a two-step sea-level rise, as indicated by the d/p ratios and MS. The d/p ratios suggest that the highest sea level observed in the MTMY-1 record is also reached at ca. 6 Ma (Fig. 4). This coincides with the timing of a global 3rd order sea level high (Handerbol et al., 1998; Fig. 4).

Late Messinian and the Messinian Salinity Crisis (ca. 5.95 – 5.33 Ma)

A very strong cooling and arid event, evidenced by a significant decrease in thermophilous taxa (from 6 to 0%) and *Quercus* (from about 25 to 0%) and an associated glacio-eustatic sea level drop, deduced from the d/p ratios and MS, is observed centered at ca. 5.95 Ma in the MTMY-1 core (Fig. 4). The intensity of the change, shown in all the studied proxies, is one of the greatest in the studied sequence, and the change from warm-wet to cold-dry seems to happen in less than 50 ka (Fig. 4).

This glaciation observed in the MTMY-1 core coincides with the timing of a strong cold event recorded in high-resolution $\delta^{18}O$ isotope records from DSDP 552A and ODP 926 and 1085 sites, which is named TG32 in literature (Keigwin, 1987; Shackleton and Hall, 1997; Vidal et al., 2002; Fig. 4). Regionally, this also coincides with the record of cold micromammal fauna in southern Spain (García-Alix et al., 2008). Related to this glaciation is a glacio-eustatic sea level drop that is observed in the MTMY-1 d/p and MS records and seems to have also triggered a 4th order low sea level detected in the western Mediterranean area (Esteban et al., 1996; Martín and Braga, 1996; Cornée et al., 2004), the final closure of the Rifian Corridors (Krijgsman et al., 1999b) and the beginning of a long period of new African-Iberian exchanges in mammal fauna (Agustí et al., 2006; Fig. 4). This also roughly coincides with the onset of evaporite deposition in Sicily, at ca. 6 Ma (Blanc-Valleron et al., 2002).

Glacio-eustatism has been recently rejected as the main cause of the MSC, as the two strongest cold stages (TG22 and TG20; ca. 5.8 Ma; Shackleton and Hall, 1997) post-date the onset of the evaporite deposition by at ca. 200 ka (Krijgsman et al., 1999a; Hodell et al., 2001; Vidal et al., 2002). However, this study, together with several above-mentioned evidences, show that previous cold periods centered at ca. 6.3 and 5.95 Ma were also very strong, producing sea-level drops estimated from a few tens of meters up to 80 – 100 m (Aharon et al., 1993; Zhang and Scott, 1996; Hodell et al., 2001; Blanc-Valleron et al., 2002; Rouchy and Caruso, 2006). In the MTMY-1 core, Pérez-Asensio et al. (2012) related a sea level drop of about 227 m with the onset of the MSC. Rohling et al. (2008) show that even smaller glacioeustatic fluctuations could have controlled the Atlantic-Mediterranean water exchange and the deposition of evaporites with shallow Atlantic-Mediterranean gateways as a result of the ongoing tectonic uplift. For example, small sea-level fluctuations of the order of 5 to 10 m with a gateway of about 50 m may have controlled the evaporite-marl cycles in the Mediterranean (Rohling et al., 2008). It is worth noticing that the cooling, and associated sea level drop, at ca. 5.95 Ma is particularly well expressed in the palynological record of the MTMY-1 core and is comparable in magnitude than the later ca. 5.8 Ma TG22-20 cold event. In short, we suggest that the onset of the MSC could have been triggered by a significant glacio-eustatic sea level drop at ca. 5.95 Ma, under a scenario of favourable tectonic boundary conditions.

Warmer temperatures are observed later on in the MTMY-1 core, with a fast recovery of thermophilous taxa and *Quercus*, peaking around 5.85 Ma. This warming is paralleled by a transgression, observed in the d/p ratios (Fig. 4), and is also observed in the marine isotopic records (Shackleton and Hall, 1997; Vidal et al, 2002). This transgression agrees with evidences of a 4^{th} order highstand observed in the western Mediterranean (Esteban et al., 1996).

A strong temperature, humidity and sea level drop are recorded later on, at ca. 5.8 Ma in the MTMY-1 record (Fig. 4). This is most likely related with global increases in ice volume, the TG22-20 cold events (Hodell et al., 1994, 2001; Shackleton and Hall, 1997; Shackleton et al., 1999a; Vidal et al., 2002), and a significant global sea level drop (Me-2; Handerbol et al., 1998), also recorded in the western Mediterranean (Esteban et al., 1996). Rouchy and Caruso (2006) relate this sea level drop, which caused the major restriction of the Atlantic-Mediterranean water exchanges, with the precipitation of K–Mg salt in Sicily.

Environmental variations (mostly d/p ratios and MS) seem to be muted since 5.8 Ma in our record (Fig. 4) and relatively low sea level is recorded. This is due to the significant regression occurred at the time of events TG22-20 (Pérez-Asensio et al., 2012), inducing significant paleogeographical changes in the Guadalquivir Basin (Sierro et al., 1996). However, some interesting cyclical variability can still be observed (see chapter below), which is coeval with pollen variations. Temperature and precipitation then show significant variability but are characterized by a decreasing trend until 5.6-5.5 Ma in the MTMY-1 record, when two minima are reached. These two cold/arid events could be tentatively related to cold events TG14 and TG12 recorded in the isotopic records (Hodell et al., 1994; Shackleton et al., 1995; Shackleton and Hall, 1997; Vidal et al., 2002). These cold events might have contributed to the final isolation and desiccation of the Mediterranean (Hodell et al., 2001; Hilgen et al., 2007). There are many regional evidences of a significant sea level drop at that time, producing erosion in the deep Mediterranean Basin (Clauzon et al., 1996), a hiatus between the Lower and Upper Evaporites (Krijgsman et al., 1999a; Fig. 4; Hilgen et al., 2007) and angular unconformities at marginal settings (Braga and Martín, 1992; Butler et al., 1995; Martín and Braga, 1994; Riding et al., 1998; Braga et al., 2006; Roveri and Manzi, 2006).

Krijgsman and Meijer (2008) suggest that the massive halite deposits from the deep Mediterranean could be linked to these cold events.

Relatively warmer and more humid climate is recorded after 5.5 Ma in the MTMY-1 record, reaching a maximum in *Quercus* at ca. 5.3 Ma. This warming trend is also recorded in many isotopic records (Hodell et al., 1994; Shackleton et al., 1995; Shackleton and Hall, 1997; Vidal et al., 2002). It is interesting to note that the end of the evaporite deposition in the Mediterranean coincides with this warming and transgression. This is consistent with the post-evaporitic sedimentary record in the Sorbas and Almería-Níjar basins, (SE Spain), where a sea-level rise ended the gypsum deposition in this marginal basins and sediments with marine organisms (*Porites* coral reefs, plancktic and benthic foraminifers, echinoderms, fishes, and so for) started to be deposited well before the Messinian/Pliocene boundary (Riding et al., 1991; Braga and Martín, 1992; Martín et al., 1993; Martín and Braga, 1994; Riding et al., 1998; Saint-Martin et al., 2000; Goubert et al., 2001; Aguirre, and Sánchez-Almazo, 2004; Braga et al., 2006). This also agrees with several other authors, who link the end of the MSC with this rise in sea level (Clauzon et al., 1996; Suc et al., 1997; McKenzie, 1999; McKenzie et al., 1999). However, many other authors reject this hypothesis arguing diachronism between this warm event and the astronomically dated end of the MSC (Hilgen et al., 2007; Vidal et al., 2002).

Cyclical changes in climate, vegetation and eustatism

Some authors have suggested that the onset of the MSC is out of phase with Milankovitch sea-level variations (Hodell et al., 2001; van der Laan et al., 2005; Govers, 2009). This is one of the main reasons why eustatic changes have been excluded as trigger for the onset of the MSC (Krijgsman et al., 1999a). However, the onset of the

MSC not only falls around a 400-ka eccentricity minimum centered ca. 6.0 Ma, but coincides strikingly with a prominent 100-ka eccentricity minima (Fig. 4). Evidences for sea level changes related to eccentricity cycles are abundant (Vail et al., 1991; Kroon et al., 2000; Gale et al., 2002) – it is, in fact, one of the most significant spectral peaks for the late Miocene both in deep-water marine sequences (i.e., site 926; Shackleton and Crowhurst, 1997 or site 1085; Vidal et al., 2002) and in reefal shelf carbonates (Braga and Martín, 1996). This reinforces the idea that long-term orbital cycle forcing, and not only obliquity, could have also played a critical role in the exact timing for the onset of the MSC (Krijgsman et al., 1999a).

Spectral analyses of the pollen record from the MTMY-1 core show cyclical changes in the vegetation (i.e., cold-dry/warm-wet) through spectral peaks at ca. 400-200, 105 and 43 ka related to eccentricity (long- and short-term) and obliquity cycles (Fig. 6). The spectral analysis and sinusoidal curve fitting show that the significant changes in vegetation are mostly forced by the long-term (400-ka) eccentricity cycle and cold events at ca. 6.3, 5.95 and 5.6 Ma, observed in the MTMY-1 record and elsewhere (see above), are mostly due to this forcing (Figs. 4 and 6). Sea level drops recorded in the MTMY-1 record, including the one at ca. 5.95 Ma, are contemporaneous with these coolings and therefore are interpreted here to have a glacio-eustatic origin. Therefore, this study shows that the onset of the MSC could be due to a significant cooling, increasing aridity, and a glacio-eustatic sea-level drop generating restriction, related to eccentricity minima (Fig. 4).

CONCLUSIONS

Pollen, dinocyst and magnetic susceptibility analyses have been carried out on a core taken from the lower Guadalquivir Basin (southwestern Spain) in an effort to understand vegetation, eustatic and climatic changes during the late Miocene in the Atlantic side of the Gibraltar Arch.

The pollen record indicates overall warm (i.e, subtropical) and arid climate for the late Miocene in this area, agreeing with previous studies. However, important changes in the abundance of *Quercus* and thermophilous taxa indicate cyclical warm-wet/cold-dry climate changes during the late Miocene in this area and strong cold and arid events are observed at ca. 7.3-7.0, 6.3, 5.95 and 5.6-5.5 Ma. Statistical analyses show that vegetation and climate were mostly forced by long-term eccentricity and the observed cold and arid events seem to coincide with 400-ka eccentricity minima. Significant sea level drops, indicated by d/p ratios and MS, appear to also occur during those cold periods and thus are interpreted here as glacio-eustatic sea level changes. Several previous studies show that sea level drops produced increasing restriction between the Atlantic and Mediterranean. One of the strongest coolings and sea level drops as inferred from the palynomorphs in the studied core occurred at ca. 5.95 Ma and could have triggered, at least in part, the onset of the MSC.

ACKNOWLEDGEMENTS

The author's research was funded by the research grants CGL-2007-60774/BTE and CGL-2010-20857/BTE by the Spanish Ministry of Science and Education, and the Research Group RNM-190 of the Junta de Andalucía (Spain). JNPA was funded by a research scholarship provided by the Spanish Ministry of Education (F.P.U. scholarship, ref. AP2007-00345). We also would like to thank two anonymous reviewers and the editor for very constructive comments on a previous version of the manuscript.

REFERENCES CITED

Aguirre, J., 1992, Evolución de las asociaciones fósiles del Plioceno marino de Cabo Roche (Cádiz): Revista Española de Paleontología, v. Extra, p. 3−10.

Aguirre, J., 1995, Implicaciones paleoambientales y paleogeográficas de dos discontinuidades estratigráficas en los depósitos pliocénicos de Cádiz (SW de España): Revista de la Sociedad Geológica de España, v. 8, p. 161−174.

Aguirre, J., and Sánchez-Almazo, I.M., 2004, The Messinian post-evaporitic deposits of the Gafares area (Almería, SE Spain). A new view of the “Lago-Mare” facies: Sedimentary Geology, v. 168, p. 71-95.

Aguirre, J., Braga, J .C., and Martín, J.M., 2007, El Mioceno marino del Prebético occidental (Cordillera Bética, SE de España): historia del cierre del Estrecho Norbético, *in* Aguirre, J., Company, M., and Rodríguez-Tovar, F.J., eds., XIII Jornadas de la Sociedad Española de Paleontología: Guía de Excursiones. Instituto Geológico y Minero de España-Universidad de Granada, Granada, p. 53−66.

Aguirre, J., Castillo, C., Férriz, F.J., Agustí, J., and Oms, O., 1995, Marine-continental magnetobiostratigraphic correlation of the Dolomys subzone (middle of Late Pliocene): implications for the Late Ruscinian age: Palaeogeography, Palaeoclimatology, Palaeoecology, v. 117, p. 139−152.

Agustí, J., Garcés, M., and Krijgsman, W., 2006, Evidence for African-Iberian exchanges during the Messinian in the Spanish mammalian record: Palaeogeography, Palaeoclimatology, Palaeoecology, v. 238, p. 5-14.

Aharon, P., Goldstein, S.L., Wheeler, C.W., and Jacobson, G., 1993, Sealevel events in the South Pacific linked with the Messinian salinity crisis: Geology, v. 21, p. 771–775.

Baceta, J.I., and Pendón, J.G., 1999, Estratigrafía y arquitectura de facies de la

Formación Niebla, Neógeno superior, sector occidental de la Cuenca del Guadalquivir: Revista de la Sociedad Geológica de España, v. 12, p. 419−438.

Bellanca, A., Caruso, A., Ferruzza, G., Neri, R., Rouchy, J.M., Sprovieri, M., and Blanc-Valleron, M.M., 2001, Transition from marine to hypersaline conditions in the Messinian Tripoli Formation from the marginal areas of the central Sicilian Basin: Sedimentary Geology, v. 140, p. 87-105.

Blanc-Valleron, M.M., Pierre, C., Caulet, J.P., Caruso, A., Rouchy, J.-M., Cespuglio, G., Sprovieri, R., Pestrea, S., and Di Stefano, E., 2002, Sedimentary, stable isotope and micropaleontological records of paleoceanographic change in the Messinian Tripoli Formtaion (Sicily, Italy): Palaeogeography, Palaeoclimatology, Palaeoecology, v. 185, p. 255-286.

Borradaile, G., Keeler, W., Aldford, C., and Sarvas P., 1987, Anisotropy of magnetic susceptibility – susceptibility of some metamorphic minerals: Physics of the Earth and Planetary Interiors, v. 48, p. 161–166.

Braga, J.C., and Martín, J.M., 1992, Messinian carbonates of the Sorbas basin: sequence stratigraphy, cyclicity and facies, in: Late Miocene carbonate sequences of southern Spain: A guidebook for the Las Negras and Sorbas Areas. SEPM/IAS Research Conference on Carbonate Stratigraphic Sequences: Sequence Boundaries and Associated Facies, August 30-September 3, La Seu, Spain, p. 78-108.

Braga, J.C., and Martín, J.M., 1996, Geometries of reef advance in response to relative sea-level changes in a Messinian (uppermost Miocene) fringing reef (Cariatiz reef, Sorbas Basin, SE Spain): Sedimentary Geology, v. 107, p. 61−81.

Braga, J.C., Martín, J.M., and Aguirre, J., 2002, Tertiary. Southern Spain, *in* Gibbons, W., and Moreno, T., eds., The Geology of Spain. The Geological Society, London, p. 320−327.

Braga, J.C., Martín, J.M., Aguirre, J., Baird, C.D., Grunnaleite, I., Jensen, N.B., Puga-Bernabéu, A., Saelen, G., and Talbot, M.R, 2010, Middle-Miocene (Serravallian) temperate carbonates in a seaway connecting the Atlantic Ocean and the Mediterranean Sea (North Betic Strait, S Spain): Sedimentary Geology, v. 225, p. 19−33.

Braga, J.C., Martín, J.M., Riding, R., Aguirre, J., Sánchez-Almazo, I.M., and Dinarès-Turell, J., 2006, Testing models for the Messinian salinity crisis: The Messinian record in Almería, SE Spain: Sedimentary Geology, v. 188−189, p. 131−154.

Butler, R.W.H., Lickorish, W.H., Grasso, M., Pedley, H.M., and Ramberti, L., 1995, Tectonics and sequence stratigraphy in Messinian Basins, Sicily: constraints on the initiation and termination of the Mediterranean salinity crisis: Geological Society of America Bulletin, v. 107, p. 425–439.

Caruso, A., 1999, Biostratigrafia, Ciclostratigrafia e Sedimentologia dei Sedimenti Tripolacei e Terrigeni del Messiniano Inferiore, A⁄oranti nel Bacino di Caltanissetta (Sicilia) en el Bacino di Lorca (Spagna): PhD Thesis, Palermo- Napoli, University, Palermo.

Civis. J., Sierro, F.J., González-Delgado, J.A., Flores, J.A., Andrés, I., de Porta, J., and Valle, M.F., 1987, El Neógeno marino de la provincia de Huelva: Antecedentes y definición de las unidades litoestratigráficas, *in* Civis, J. ed., Paleontología del Neógeno de Huelva. Ediciones Universidad de Salamanca, Salamanca, p. 9−21.

Clauzon, G., Suc, J.-P., Gautier, F., Berger, A., and Loutre, M.-F., 1996, Alternate interpretation of the Messinian salinity crisis: controversy resolved?: Geology, v. 24, p. 363–366.

Collinson, D.W., 1983, Methods in Rock Magnetism and Palaeomagnetism. Techniques and Instrumentation: Chapman and Hall, London, 503 pp.

Cornée, J.-J., Saint Martin, J.-P., Conesa, G., Munch, P.H., André, J.-P., Saint Martin, S., and Roger, S., 2004, Correlations and sequence stratigraphic model for Messinian carbonate platforms of the western and central Mediterranean: International Journal of Earth Sciences, v. 93, p. 621–633.

Esteban, M., Braga, J.C., Martín, J.M., and Santisteban, C., 1996, Western Mediterranean reef complexes, *in* Franseen, E.K., Esteban, M., Ward, W.C., and Rouchy, J.M., eds., Models for Carbonate Stratigraphy from Miocene Reef Complexes of Mediterranean Regions. SEPM, Concepts in Sedimentology and Paleontology v. 5, p. 55–72.

Evans, M.E., and Heller, F., 2003, Environmental magnetism. Principles and applications of enviromagnetics: Academic Press, 299 pp.

Faegri, K., and Iversen, J., 1989, Textbook of Pollen Analysis: Wiley, New York.

Fauquette, S., Suc, J.-P., Bertini, A., Popescu, S.-M., Warny, S., Bachiri Taoufiq, N., Perez Villa, M.-J., Chikhi, H., Subally, D., Feddi, N., Clauzon, G., and Ferrier, J., 2006, How much did climate force the Messinian salinity crisis? Quantified climatic conditions from pollen records in the Mediterranean region: Palaeogeography, Palaeoclimatology, Palaeoecology, v. 238, p. 281–301.

Fernández, M., Berástegui, X., Puig, C., García-Castellanos, D., Jurado, M.J., Torné, M., and Banks, C., 1998, Geophysical and geological constraints on the evolution of the Guadalquivir foreland basin, Spain *in* Mascle, A., Puigdefàbregas, C., Luterbacker, H.P., and Fernández, M., eds., Cenozoic Foreland Basins of Western Europe. Geological Society Special Publication, v. 134, p. 29–48.

Fletcher, W.J., and Sánchez Goñi, M.F., 2008, Orbital- and sub-orbital-scale climate impacts on vegetation of the western Mediterranean basin over the last 48,000 yr: Quaternary Research, v. 70, p. 451-464.

Fletcher, W.J., Boski, T., and Moura, D., 2007, Palynological evidence for environmental and climatic change in the lower Guadiana valley, Portugal, during the last 13000 years: The Holocene, v. 17, p. 481–494.

Fletcher, W.J., Sanchez Goñi, M.F., Peyron, O., and Dormoy, I., 2010, Abrupt climate changes of the last deglaciation detected in a Western Mediterranean forest record: Climate of the Past, v. 6, p. 245–264.

Flores, J.A., 1987, El nanoplancton calcáreo en la formación «Arcillas de Gibraleón»: síntesis bioestratigráfica y paleoecológica, *in* Civis, J., ed., Paleontología del Neógeno de Huelva. Ediciones Universidad de Salamanca, Salamanca, p. 65−68.

Gale, A.S., Hardenbol, J., Hathway, B., Kennedy, W.J., Young, J.R., and Phansalkar, V., 2002, Global correlation of Cenomanian (Upper Cretaceous) sequences: Evidence for Milankovitch control on sea level: Geology, v. 30, p. 291-294.

García-Alix, A., Minwer-Barakat, R., Martín Suarez, E., Freudenthal, M., and Martín, J.M., 2008, Late Miocene-Early Pliocene climatic evolution of the Granada Basin (southern Spain) deduced from the paleoecology of the micromammal associations: Palaeogeography, Palaeoclimatology, Palaeoecology, v. 265, p. 214-225.

González-Delgado, J.A., Civis, J., Dabrio, C.J., Goy, J.L., Ledesma, S., Pais, J., Sierro, F.J., and Zazo, C., 2004, Cuenca del Guadalquivir, *in* Vera, J.A. ed., Geología de España. SGE-IGME, Madrid, p. 543-550.

Goubert, E., Nerandeau, D., Rouchy, J.M., and Lacour, D., 2001, Foraminiferal record of environmental changes: Messinian of the Los Yesos area (Sorbas Basin, SE Spain): Palaeogeography, Palaeoclimatology, Palaeoecology, v. 175, p. 61-78.

Govers, R., 2009, Choking the Mediterranean to dehydration: the Messinian salinity crisis: Geology, v. 37, p. 167–170.

Grimm, E.C., 1987, CONISS: a FORTRAN 77 program for stratigraphically constrained cluster analysis by the method of incremental sum of squares: Computers and Geosciences, v. 13, p. 13–35.

Hammer, Ø., Harper, D.A.T., and Ryan, P.D., 2001, PAST: Paleontological Statistics Software Package for Education and Data Analysis: Palaeontologia Electronica, v. 4, p. 1-9.

Handerbol, J., Thierry, J., Farley, M.B., Jacquin, T., Graciansky, P.-C., and Vail, P.R., 1998, Mesozoic and Cenozoic sequence chronostratigraphic chart, *in* Graciansky, P.C., Handerbol, J., Jacquin, T., and Vail, P.R., eds., Mesozoic and Cenozoic Sequence Stratigraphy of European Basins, Society for Sedimentary Geology (Special Publication 60).

Haq, B.U., Hardenbol, J., and Vail, P.R., 1987, Chronology of fluctuating sea levels since the Triassic: Science v. 235, p. 1156−1167.

Heusser, L.E., 1983, Contemporary pollen distribution in coastal California and Oregon: Palynology, v. 7, p. 19–42.

Heusser, L.E., 1988, Pollen distribution in marine sediments on the continental margin of Northern California: Marine Geology, v. 80, p. 131–147.

Hilgen, F., Kuiper, K., Krijgsman, W., Snel, E., and van der Laan, E., 2007, Astronomical tuning as the basis for high resolution chronostratigraphy: the intricate history of the Messinian Salinity Crisis: Stratigraphy, v. 4, p. 231–238.

Hodell, D.A., Benson, R.H., Kent, D.V., Boersma, A., and Rakic-El Bied, K., 1994, Magnetostratigraphic, biostratigraphic, and stable isotope stratigraphy of an Upper Miocene drill core from the Sale. Briqueterie (northwestern Morocco): a high-resolution chronology for the Messinian stage: Paleoceanography, v. 9, p. 835-855.

Hodell, D.A., Curtis, J.H., Sierro, F.J., and Raymo, M.E., 2001, Correlation of late Miocene to early Pliocene sequences between the Mediterranean and North Atlantic:

Paleoceanography, v. 16, p. 164-178.

Iaccarino, S.M., Bertini, A., Di Stefano, A., Ferraro, L., Gennari, R., Grossi, F., Lirer, F., Manzi, V., Menichetti, E., Ricci Lucchi, M., Taviani, M., Sturiale, G., and Angeletti, L., 2008, The Trave section (Monte dei Corvi, Ancona, Central Italy): an integrated paleontological study of the Messinian deposits: Stratigraphy, v. 5 (3-4), p. 281-306.

Jiménez-Moreno, G., Rodríguez-Tovar, F.-J., Pardo-Igúzquiza, E., Fauquette, S., Suc, J.-P., and Müller, P., 2005, High-resolution palynological analysis in late early-middle Miocene core from the Pannonian Basin, Hungary: climatic changes, astronomical forcing and eustatic fluctuations in the Central Paratethys: Palaeogeography, Palaeoclimatology, Palaeoecology, v. 216 (1–2), p. 73–97.

Jiménez-Moreno, G., Head, M.J., and Harzhauser, M., 2006, Early and Middle Miocene dinoflagellate cyst stratigraphy of the Central Paratethys, Central Europe: Journal of Micropaleontology, v. 25, p. 113-139.

Jiménez-Moreno, G., Fauquette, S., and Suc, J.-P., 2008, Vegetation, climate and paleoaltitude reconstructions of eastern alpine mountain ranges during the Miocene based on pollen records from Austria, Central Europe: Journal of Biogeography, v. 35, p. 1638-1649.

Jiménez-Moreno, G., Suc, J.-P., and Fauquette, S., 2010, Miocene to Pliocene vegetation reconstruction and climate estimates in the Iberian Peninsula from pollen data: Review of Palaebotany and Palynology, v. 162, p. 403-415.

Kastens, K. A., 1992, Did a glacio-eustatic sea level drop trigger the Messinian Salinity crisis? New evidence from Ocean Drilling Program site 654 in the Tyrrhenian Sea: Paleoceanography, v. 7, p. 333-356.

Keigwin, L. D., Jr., 1987, Toward a high-resolution chronology for latest Miocene paleoceanographic events: Paleoceanography, v. 2, p. 639-660.

Krijgsman, W., Hilgen, F.J., Raffi, I., Sierro, F.J., and Wilson, D.S., 1999a, Chronology, causes and progression of the Messinian Salinity Crisis: Nature, v. 400, p. 652-655.

Krijgsman, W., Langereis, C.G., Zachariasse, W.J., Boccaletti, M., Moratti, G., Gelati, R., Iaccarino, S., Papani, G., and Villa, G., 1999b, Late Neogene evolution of the Taza-Guercif basin (Rifian Corridor, Morocco) and implications for the Messinian salinity crisis: Marine Geology, v. 153, p. 147-160.

Kroon, D., Williams, T., Pirmez, C., Spezzaferri, S., Sato, T., and Wright, J.D., 2000, Coupled early Pliocene–middle Miocene bio-cyclostratigraphy of Site 1006 reveals orbitally induced cyclicity patterns of Great Bahama Bank carbonate production: Proc. ODP Sci. Results, v. 166, p. 155–166.

Larrasoaña, J.C., González-Delgado, J.A., Civis, J., Sierro, F.J., Alonso-Gavilán, G., and Pais, J., 2008, Magnetobiostratigraphic dating and environmental magnetism of Late Neogene marine sediments recovered at the Huelva-1 and Montemayor-1 boreholes (lower Guadalquivir basin, Spain): Geo-Temas, v. 10, p. 1175−1178.

Larsen, H.C., Saunders, A.D., Clift, P.D., Beget, J., Wei, W., Spezzaferri, S., and ODP Leg 152 Scientific Party, 1994, Seven million years of glaciation in Greenland: Science, v. 264, p. 952-955.

Laskar, J., Robutel, P., Joutel, F., Gastineau, M., Correia, A.C.M., and Levrard, B., 2004, A long term numerical solution for the insolation quantities of the Earth: Astronomy and Astrophysics, v. 428, p. 261-285.

Lear, C.H., Rosenthal, Y., and Wright, J.D., 2003, The closing of a seaway: ocean water masses and global climate change: Earth and Planetary Science Letters, v. 210, p. 425-436.

Lourens, L.J., Hilgen, F.J., Shackleton, N.J., Laskar, J., and Wilson, D.S., 2004, The

Neogene Period, *in* Gradstein F.M., Ogg J.G., and Smith A.G., eds., A Geologic Time Scale 2004, Cambridge University Press, Cambridge, p. 409−440.

Martín, J.M., and Braga, J.C., 1994, Messinian events in the Sorbas basin in southeastern Spain and their implications in the recent history of the Mediterranean: Sedimentary Geology, v. 90, p. 257−268.

Martín, J.M., and Braga, J.C., 1996, Tectonic signals in the Messinian stratigraphy of the Sorbas basin (Almería, SE Spain), *in* Friend, P.F., Dabrio, C.J., eds., Tertiary basins of Spain: the stratigraphic record of crustal kinematics, Cambridge University Press, Cambridge, World and Regional Geology Series, v. 6, p. 387–391.

Martín, J.M., Braga, J.C., and Riding, R., 1993, Siliciclastic stromatolites and thrombolites, late Miocene, S.E. Spain: Journal of Sedimentary Petrology, v. 63, p. 131-139.

Martín, J.M., Braga, J.C., Aguirre, J., and Puga-Bernabéu, A., 2009, History and evolution of the North-Betic Strait (Prebetic Zone, Betic Cordillera): A narrow, early Tortonian, tidal-dominated, Atlantic-Mediterranean marine passage: Sedimentary Geology, v. 216, p. 80−90.

Martín, J.M., Braga, J.C., Sánchez-Almazo, I.M., and Aguirre, J., 2010, Temperate and tropical carbonate-sedimentation episodes in the Neogene Betic basins (S Spain) linked to climatic oscillations and changes in the Atlantic-Mediterranean connections. Constraints with isotopic data, *in* Betzler, C., Mutti, M., and Piller, W., eds., Carbonate systems during the Oligocene-Miocene climatic transition, Blackwell, Oxford, International Association of Sedimentologists Special Publication, v. 42, p. 49−69.

Mayoral, E., and Pendón, J.G., 1987, Icnofacies y sedimentación en zona costera. Plioceno superior (?), litoral de Huelva: Acta Geológica Hispánica, v. 21-22, p.

507−513.

McKenzie, J.A., 1999, From desert to deluge in the Mediterranean: Nature, v. 400, p. 613-614.

McKenzie, J.A., Spezzaferri, S., and Isern, A., 1999, The Miocene/Pliocene Boundary in the Mediterranean Sea and Bahamas: Implications for a global £ooding event in the Earliest Pliocene: Mem. Soc. Geol. It., v. 54, p. 93-108.

Paillard, D., Labeyrie, L., and Yiou, P., 1996, Macintosh program performs time-series analysis: Eos, v. 77, p. 379.

Pérez-Asensio, J.N., Aguirre, J., Schmiedl, G., and J. Civis, 2012, Messinian paleoenvironmental evolution in the lower Guadalquivir Basin (SW Spain) based on benthic foraminifera: Palaeogeography, Palaeoclimatology, Palaeoecology, v. 326-328, p. 135−151.

Riaza, C., and Martínez del Olmo, W., 1996, Depositional model of the Guadalquivir-Gulf of Cádiz Tertiary basin, *in* Friend, P., and Dabrio, C.J., eds., Tertiary Basins of Spain, Cambridge University Press, Cambridge, p. 330−338.

Riding, R., Braga, J.C., and Martín, J.M., 1991, Oolite stromatolites and thrombolites, Miocene, Spain: analogues of Recent giant Bahamian examples: Sedimentary Geology, v. 71, p. 121-127.

Riding, R., Braga, J.C., Martín, J.M., and Sánchez-Almazo, I.M., 1998, Mediterranean Messinian Salinity Crisis: constraints from a coeval marginal basin, Sorbas, southeastern Spain: Marine Geology, v. 146, p. 1−20.

Roberts, A.P., and Turner, G.M., 1993, Diagenetic formation of ferromagnetic iron sulphide minerals in rapidly deposited marine sediments, South Island, New Zealand: Earth and Planetary Science Letters, v. 115, p. 257–273.

Rochette, P., 1987, Magnetic susceptibility of the rock matrix related to magnetic fabric studies: Journal of Structural Geology, v. 9, p. 1015-1020.

Rohling, E.J., Schiebel, R., and Siddall, M., 2008, Controls on Messinian Lower Evaporite cycles in the Mediterranean: Earth and Planetary Science Letters, v. 275, p. 165-171.

Rouchy, J. M., and Caruso, A., 2006, The Messinian salinity crisis in the Mediterranean basin: A reassessment of the data and an integrated scenario: Sedimentary Geology, v. 188-189, p. 35-67.

Roveri, M., and Manzi, V., 2006, The Messinian salinity crisis: looking for a new paradygm?: Palaeogeography, Palaeoclimatology, Palaeoecology, v. 238, p. 386-398.

Saint-Martin, J.P., Néraudeau, D., Lauriat-Rage, A., Goubert, E., Secrétan, S., Babinot, J.F., Boukli-Hacene, S., Pouyet, S., Lacour, D., Pestrea, S., and Conesa, G., 2000, La faune interstratifiée dans les gypses messiniens de Los Yesos (bassin de Sorbas, SE Espagne): Implications: Geobios, v. 33, p. 637-649.

Salvany, J.M., Larrasoaña, J.C., Mediavilla, C., and Rebollo, A., 2011, Chronology and tectono-sedimentary evolution of the Upper Pliocene to Quaternary deposits of the lower Guadalquivir basin, SW Spain: Sedimentary Geology, v. 241, p. 22–39.

Sánchez-Almazo, I.M., Spiro, B., Braga, J.C., and Martín, J.M., 2001, Constraints of stable isotope signatures on the depositional palaeoenvironments of upper Miocene reef and temperate carbonates in Sorbas Basin, SE Spain: Palaeogeography, Palaeoclimatology, Palaeoecology, v. 175, p. 153−172.

Sánchez-Almazo, I.M., Braga, J.C., Dinarès-Turell, J., Martín, J.M., and Spiro, B., 2007, Palaeoceanographic controls on reef deposition: the Messinian Cariatiz reef (Sorbas Basin, Almería, SE Spain): Sedimentology, v. 54, p. 637–660.

Sánchez-Goñi, M.F., Landais, A., Fletcher, W.J., Naughton, F., Desprat, S., and Duprat, J., 2008, Contrasting impacts of Dansgaard-Oeschger events over a western European latitudinal transect modulated by orbital parameters: Quaternary Science Reviews, v. 27, p. 1136–1151.

Sanz de Galdeano, C., and Vera, J.A., 1992, Stratigraphic record and palaeogeographical context of the Neogene basins in the Betic Cordillera, Spain: Basin Research, v. 4, p. 21−36.

Schultz, M., and Mudelsee, M., 2002, REDFIT: estimating red-noise spectra directly from unevenly spaced paleoclimatic time series: Computers and Geosciences, v. 28, p. 421–426.

Shackleton, N.J., and Crowhurst, S., 1997, Sediment fluxes based on orbitally tuned time scale 5 Ma to 14 Ma, Site 926, *in* Shackleton, N.J., Curry, W.B., Richter, C., and Bralower, T.J., eds., Proceedings ODP Scientific Results v. 154, p. 69-82.

Shackleton, N.J., and Hall, M.A., 1997. The Late Miocene stable isotope record, Site 926, *in* Shackleton, N.J., Curry, W.B., Richter, C., and Bralower, T.J., eds., Proceedings ODP Scientific Results v. 154, p. 367–374.

Shackleton, N.J., Hall, M.A, and Pate, D., 1995, Pliocene stable isotope stratigraphy of Site 846, *in* Pisias, N.G., et al. eds., Proceedings ODP Scientific Results, v. 138, p. 5–21.

Sierro, F.J., 1985, Estudio de los foraminíferos planctónicos, bioestratigrafía y cronoestratigrafía del Mio-Plioceno del borde occidental de la cuenca del Guadalquivir (S.O. de España): Stvdia Geologica Salmanticensia, v. 21, p. 7−85.

Sierro, F.J., 1987, Foraminíferos planctónicos del Neógeno marino del sector occidental de la cuenca del Guadalquivir: síntesis y principales resultados, *in* Civis, J. ed., Paleontología del Neógeno de Huelva, Ediciones Universidad de Salamanca, Salamanca, p. 23−54.

Sierro, F.J., Flores, J.A., Civis, J., González-Delgado, J.A., and Francés, G., 1993, Late

Miocene globorotaliid event-stratigraphy and biogeography in the NE-Atlantic and Mediterranean: Marine Micropaleontology, v. 21, p. 143−168.

Sierro, F.J., González Delgado, A., Dabrio, C.J., Flores, A., and Civis, J., 1996, Late Neogene depositional sequences in the foreland basin of Guadalquivir (SW Spain), *in* Friend, P.F., and Dabrio, C.J., eds., Tertiary basins of Spain, Cambridge University Press, p. 339-345.

Suc, J.-P., and Bessais, E., 1990, Pérennité d'un climat thermoxérique en Sicile, avant, pendant et après la crise de salinité messinienne: C. R. Acad. Sci. Paris, v. 310 (2), p. 1701–1707.

Suc, J.-P., Bertini, A., Combourieu-Nebout, N., Diniz, F., Leroy, S., Russo-Ermolli, E., Zheng, Z., Bessais, E., and Ferrier, J., 1995, Structure of West Mediterranean and climate since 5,3 Ma: Acta Zoologica Cracoviensia, v. 38, p. 3–16.

Suc, J.P., Clauzon, G., and Gautier, F., 1997, The Miocene/Pliocene boundary: Present and future, *in* Montanari, A., Odin, G.S., Coccioni, R., eds., Miocene Stratigraphy: An Integrated Approach, Developments in Palaeontology and Stratigraphy, v.15, p. 149-154.

Vail, P.R., Audemard, S.A., Bowman, S.A., Eisner, P.N., and Perez-Cruz, C., 1991, The stratigraphic signatures of tectonics, eustasy and sedimentology—An overview, *in* Einsele, G., Seilacher, A., eds., Cycles and events in stratigraphy, Springer-Verlag, p. 617–662.

Van der Laan, E., Gaboardi, S., Hilgen, F.J., and Lourens, L.J., 2005, Regional climate and glacial control on high-resolution oxygen isotope records from Ain El Beida (latest Miocene, NW Morocco): a cyclostratigraphic analysis in the depth and time domain: Paleoceanography, v. 20, PA1001.

Vidal, L., Bickert, T., Wefer, G., and Röhl, U., 2002, Late Miocene stable isotope stratigraphy of SE Atlantic ODP Site 1085: relation to Messinian events: Marine Geology, v. 180, p. 71–85.

Warny, S., Bart, P.J., and Suc, J.-P., 2003, Timing and progression of climatic, tectonic and glacioeustatic influences on the Messinian Salinity Crisis: Palaeogeography, Palaeoclimatology, Palaeoecology, v. 202, p. 59–66.

Weijermars, R., 1988, Neogene tectonics in the Western Mediterranean may have caused the Messinian Salinity Crisis and an associated glacial event: Tectonophysics, v. 148, p. 211−219.

Zachos, J.C., Pagani, M., Sloan, L., Thomas, E., and Billups, K., 2001, Trends, rhythms, and aberrations in global climate 65 Ma to present: Science, v. 292, p. 686–693.

Zhang, J., and Scott, D.B., 1996, Messinian deep-water turbidites and glacioeustatic sea-level changes in the North Atlantic: linkage to the Mediterranean salinity crisis: Paleoceanography, v. 11, p. 277–297.

Zheng, Z., Huang, K.Y., Xu, Q.H., Lv, H.Y., Cheddadi, R., Luo, Y.L., Beaudouin, C., Luo, C.X., Zheng, Y.W., Li, C.H., Wei, J.H., and Du, C.B., 2008, Comparison of climatic threshold of geographical distribution between dominant plants and surface pollen in China: Science China Series D, v. 51, p. 1107–1120.

Figure Captions

Figure 1. (Top) Geological framework of southern Spain. In white is the Atlantic Neogene Guadalquivir Basin. (Bottom) The star marks the location of the MTMY-1

core near Moguer, southern Spain.

Figure 2. Age-depth model for the MTMY-1 record (modified after Larrasoaña et al., 2008). On the left is the synthetic lithology of the core and the paleomagnetic properties of the sediments [Magnetic Susceptibility (MS), Normal Remanescent Magnetisation (NRM) and inclination]. Arrows mark the location of biostratigraphic events recognized by planktonic foraminifera (Sierro et al., 1996). Dashed lines indicate the interpreted correlation to the ATNTS04 (Lourens et al., 2004). Main events related with the MSC are also indicated.

Figure 3. Detailed pollen diagram and dinocyst abundance of the MTMY-1 core. Only species with percentages higher than 1% are shown. In green and yellow are the non-coniferous trees and herbs respectively. On the right, a cluster analysis (Grimm, 1987) of the pollen results and pollen zones are shown.

Figure 4. Comparison of palaeoenvironmental records for the late Miocene and Pliocene (7.5 – 5.0 Ma). (A) Global sea level cycles of Handerbol et al. (1998) (light blue) and 4th order eustatic cycles distinguished in the western Mediterranean (Esteban et al., 1996; darker blue). The main cycle boundaries are shown for both curves. (B) Magnetic susceptibility (MS) for the MTMY-1 core. (C) Total *Quercus* and thermophilous taxa (Arecaceae, *Acacia*, *Avicennia*, Chloranthaceae, *Eucommia*, Menispermaceae, *Alchornea*-type, Rutaceae, *Parthenocissus*, *Prosopis*, *Engelhardia*, *Platycarya*, *Symplocos*, *Myrica*, Taxodiaceae, Sapotaceae, Celastraceae, *Microtropis fallax*, Rubiaceae and *Mussaenda*) percentages for the MTMY-1 core. Major isotopic events (Hodell et al., 1994; Vidal et al., 2002) and trends are indicated. (D) MTMY-1

d/p ratios. (E) $\delta^{18}O$ in benthic foraminifera record from ODP Site 926 (Shackleton and Hall, 1997). (F) Filtered 400- and 100-ka components of orbital eccentricity (Laskar et al., 2004). (G) Main Mediterranean events (Krijgsman et al., 1999a). (H) Timing for Africa-Iberian mammal exchanges (Agustí et al., 2006).

Figure 5. Correlation between the d/p ratios and MS for the 4.5 – 7.3 Ma interval of the MTMY-1 record. In order to make this correlation, new sampling every 0.03 Ma was carried out on both records using Analyseries (Paillard et al., 1996). The R^2 value is shown.

Figure 6. Spectral analyses of the total *Quercus* pollen time series from the MTMY-1 core. (A) Spectral analysis of the 5.0 – 6.5 Ma interval. (B) A 400-ka sinusoidal curve fitting on the total *Quercus* pollen data. (C) Spectral analysis of the higher-resolution 5-6 Ma interval showing statistically significant spectral peaks.

Table 1. Age data for MTMY-1 core, southern Spain.

Figure 1

Click here to download Figure: Fig. 1. Jimenez-Moreno et al.eps

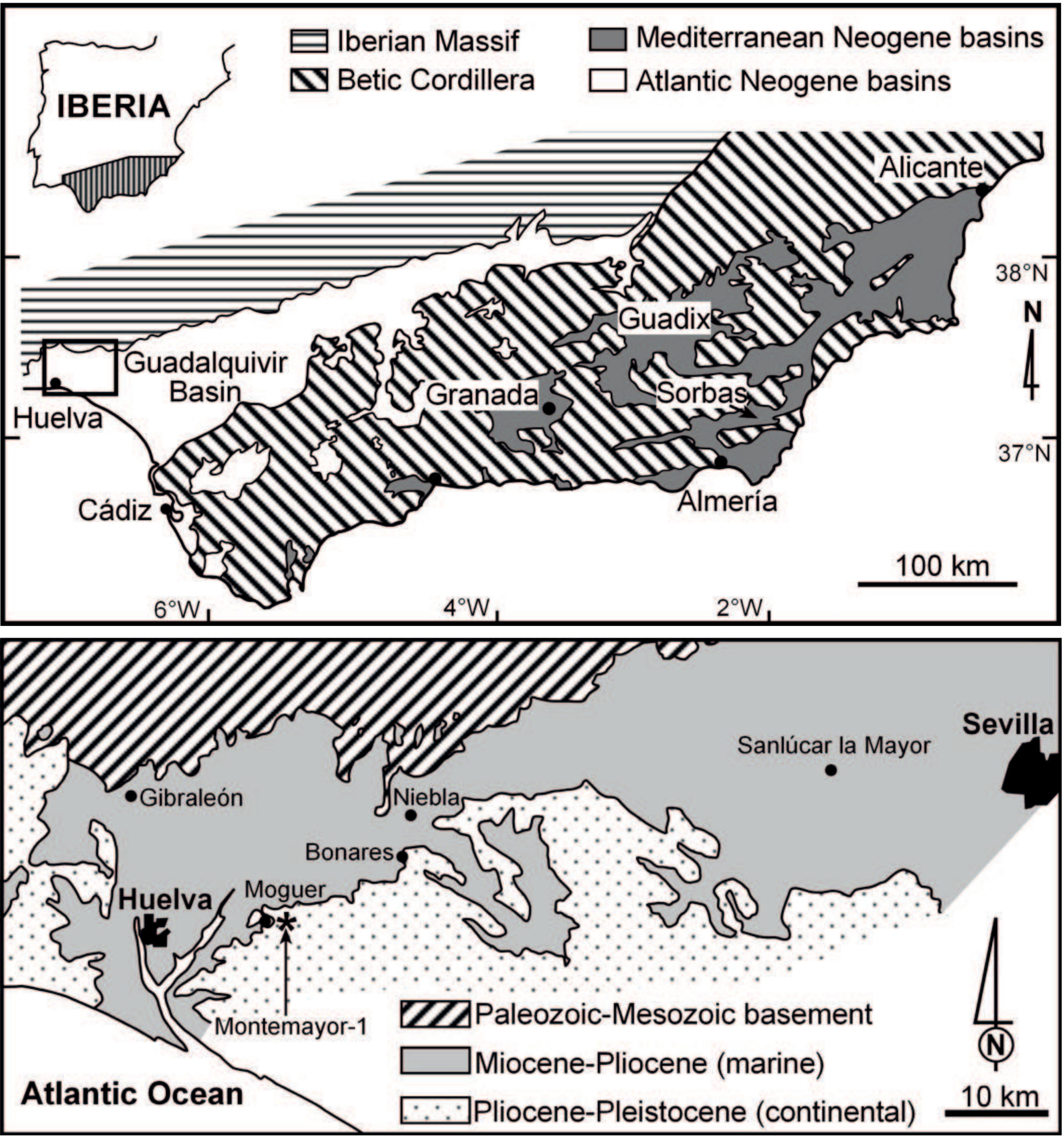

Figure 2

Click here to download Figure: Fig. 2. Jimenez-Moreno et al.eps

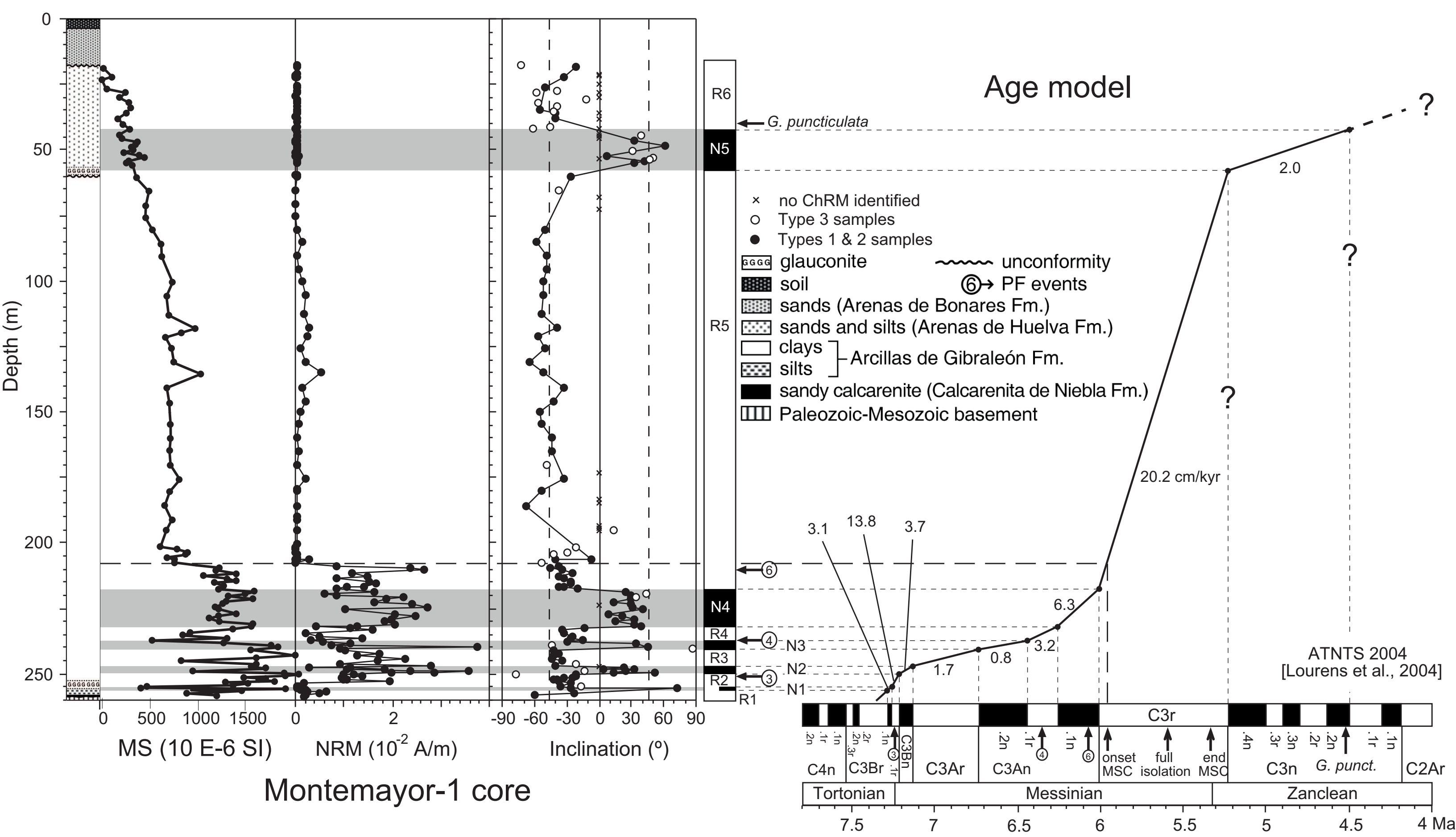

Figure 3

Click here to download Figure: Fig. 3. Jimenez-Moreno et al.eps

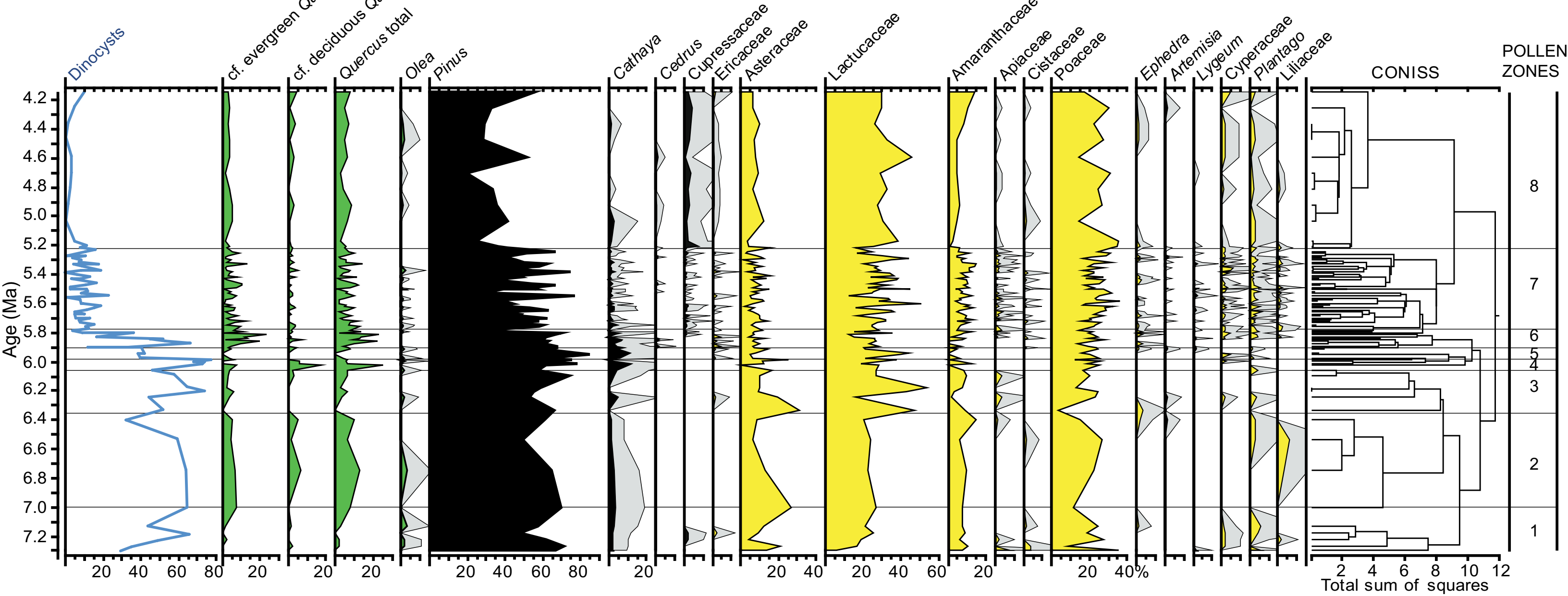

Figure 4
Click here to download Figure: Fig. 4. Jimenez-Moreno et al.eps

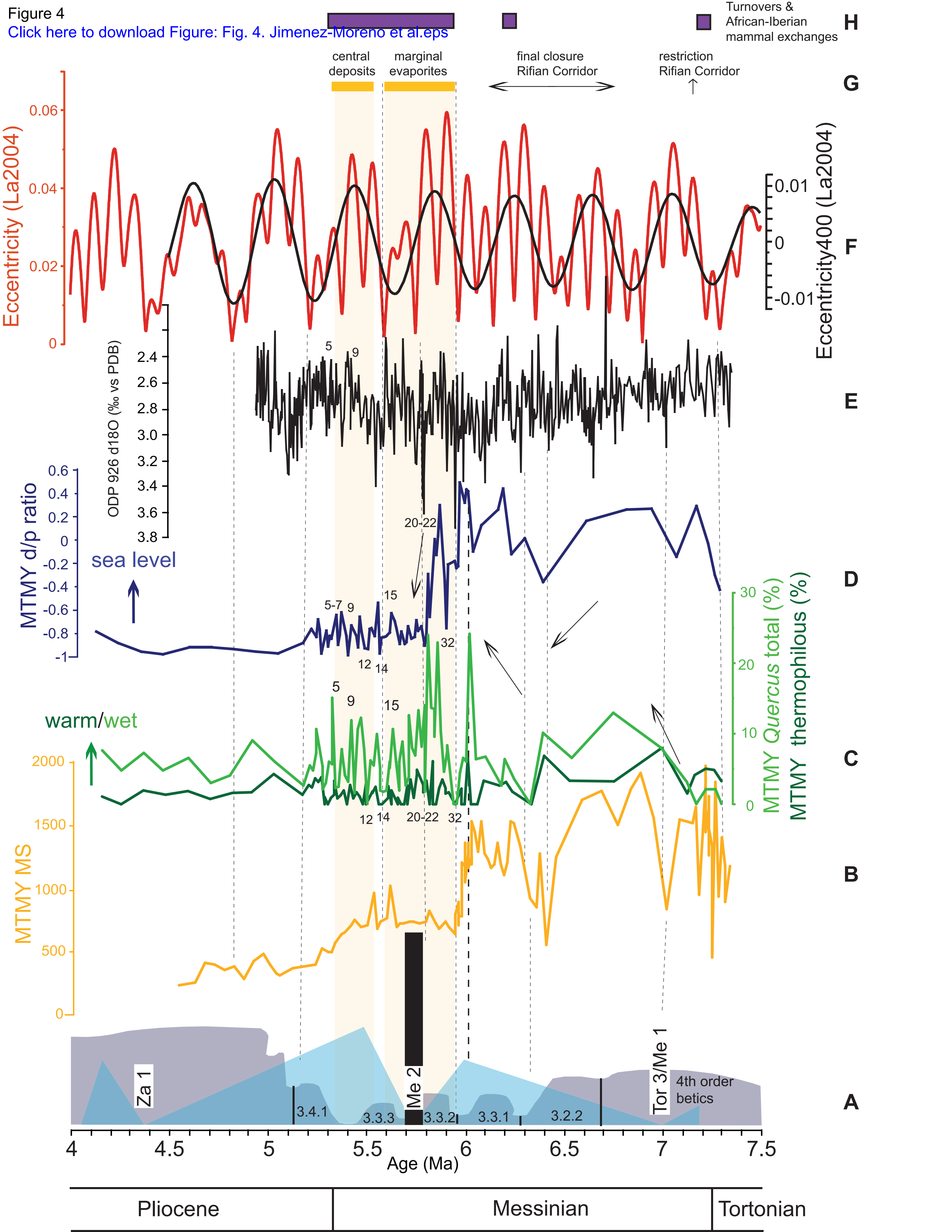

Figure 5

Click here to download Figure: Fig. 5. Jimenez-Moreno et al.eps

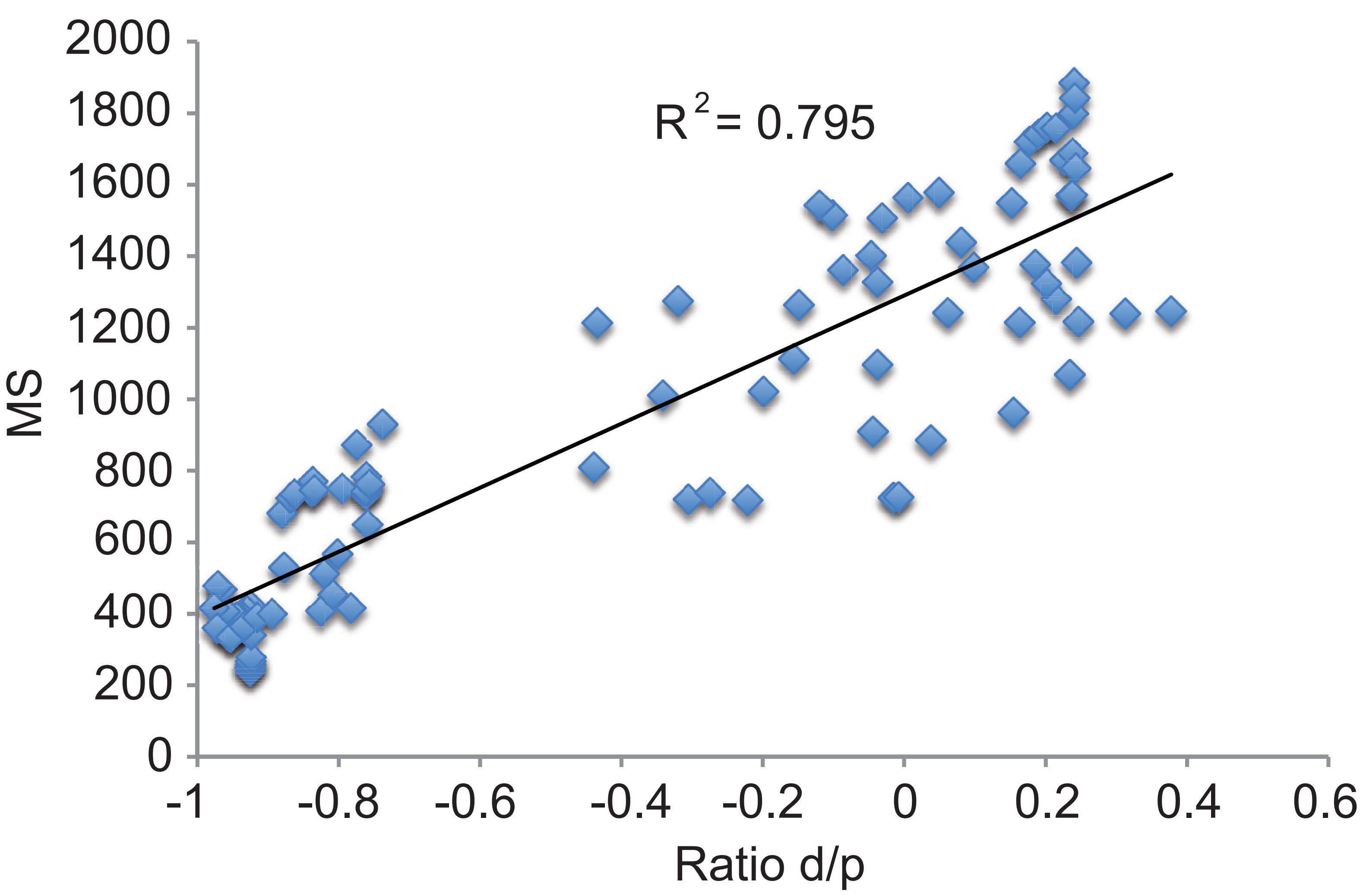

Figure 6
Click here to download Figure: Fig. 6. Jimenez-Moreno et al.eps

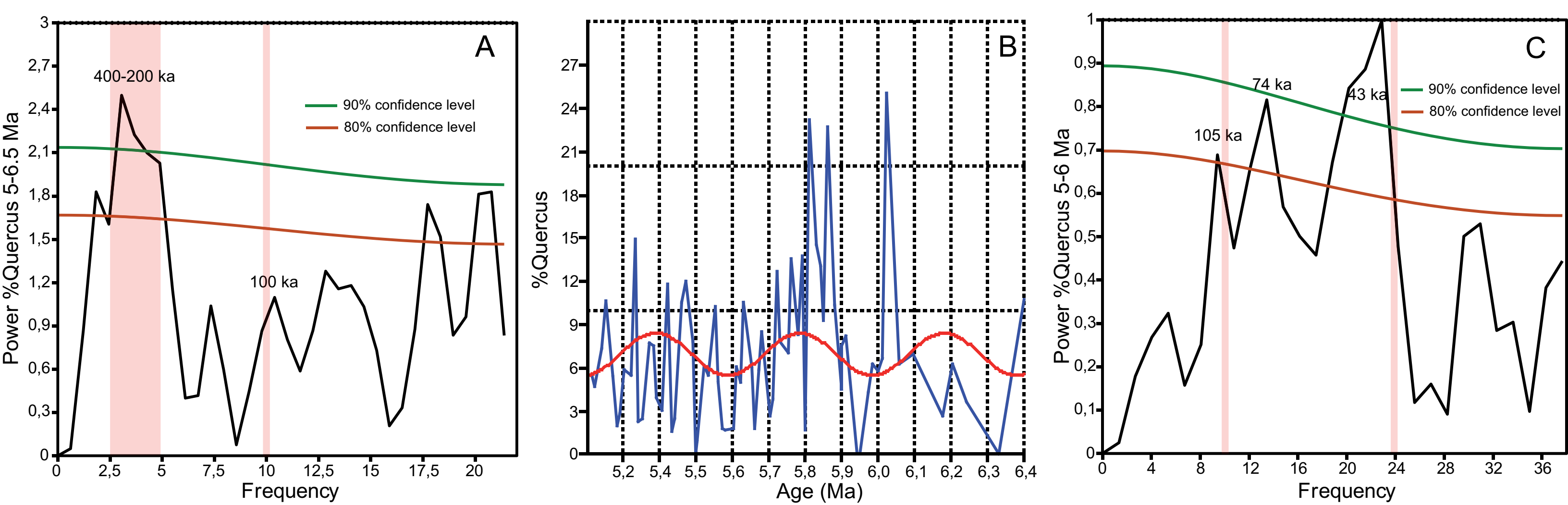

Table 1

Table 1. Age model for the MTMY core.

Datum	Depth	Age Ma (ATNTS 2004)	MAR (cm/kyr)
C3n.2n top	42.35	4.493	2.0
C3n.4n base	57.45	5.235	20.2
C3An.1n top	218.30	6.033	6.3
C3An.1n base	232.15	6.252	3.2
C3An.2n top	238.10	6.436	0.8
C3An.2n base	240.40	6.733	1.7
C3Bn top	247.30	7.140	3.7
C3Bn top	250.00	7.212	13.8
C3Br.1n top	255.40	7.251	3.1
C3Br.1n base	256.45	7.285	